Revisiting freely decaying two-dimensional turbulence at millennial resolution

A. Bracco[a)]
Istituto di Cosmogeofisica del CNR, corso Fiume 4, I-10133 Torino, Italy

J. C. McWilliams
Institute of Geophysics and Planetary Physics, University of California at Los Angeles, Los Angeles, California 90095-1567

G. Murante
Osservatorio Astronomico di Torino, I-10025, Pino T.se, Italy

A. Provenzale
Istituto di Cosmogeofisica del CNR, corso Fiume 4, I-10133 Torino, Italy

J. B. Weiss
PAOS, University of Colorado, Boulder, Colorado 80309

(Received 28 October 1999; accepted 12 July 2000)

We study the evolution of vortex statistics in freely decaying two-dimensional turbulence at very large Reynolds number. The results obtained here confirm that the peak vorticity inside vortex cores is conserved and that the number of vortices as a function of time, $N(t)$, decreases as a power law. In addition, the numerical findings are consistent with the predictions of the scaling theories proposed by Carnevale *et al.* [Phys. Rev. Lett. **66**, 2735 (1991)] and Weiss and McWilliams [Phys. Fluids A **5**, 608 (1993)]. We also obtain new evidence for a self-similar distribution of vortex radii and circulations, that suggests the possibility of a generic statistical behavior of the decaying phase of two-dimensional turbulence at high Reynolds number. © *2000 American Institute of Physics.* [S1070-6631(00)50711-9]

I. INTRODUCTION

In recent years, the behavior of two-dimensional (2D) turbulence has been widely investigated, due to its interest as a simple conceptual model of vortex-dominated large-scale planetary flows.[1,2]

Two-dimensional turbulent flows at high Reynolds number, (Re), are characterized by the spontaneous emergence of coherent vortices with lifetimes longer than the characteristic time scale of the nonlinear turbulent interactions.[3–7] The coherent vortices contain most of the energy and enstrophy of the system,[8] and they extend their influence to the whole field, as shown by the analysis of velocity distributions.[9,10] A low vorticity background, where strong filamentation processes take place, is observed outside the vortices.

In freely decaying 2D turbulence, coherent vortices emerge from random Gaussian initial conditions, after the time of maximum energy dissipation, whenever advective effects dominate over diffusion. How and why the fluid self-organizes into a collection of coherent elements remains a partially open question. The inverse energy cascade is thought to be at the origin of the phenomenon as it implies a significant growth of the integral scale and hence some spatial organization. The formation of the vortices is believed to be related to local axisymmetrization about a sufficiently dominant extremum, as well as to the evolutionary sequence of inflectional instabilities of the initial velocity field and roll-up of vortex sheets.

Once the vortices have formed and the *vortex generation* period is over, at intermediate times the evolution proceeds through mutual vortex advection and strong inelastic interactions of same-sign vortices.[3,11,12] At very late times, systems with zero average vorticity in bounded domains tend to a final state consisting of a vortex dipole at the largest scales, which decays slowly due to dissipation.[13]

The intermediate, vortex-dominated evolution stage has been studied by several authors. A temporal scaling theory has been proposed by Carnevale *et al.*[14] and revisited by Weiss and McWilliams[15] with the addition of finite Reynolds number corrections. According to this theory, the vortex properties display self-similar behavior in time. In particular, average quantities such as the vortex number and the average vortex radius have a power-law dependence on time. Moreover, all the decay rates are expressed in terms of a single fundamental exponent. The inferences drawn from the scaling theory were shown to agree with the results of numerical simulations of 2D turbulence and point-vortex systems[15] and with laboratory experiments.[16]

In later work, however, the above results were claimed to be dominated by the presence of strong dissipation, being unrepresentative of the high Reynolds number limit.[17] In particular, the number of vortices that was found to be decaying with time in the scaling theory of Carnevale *et al.*,[14] was

a)Author to whom correspondence should be addressed: Electronic mail: annalisa@icg.to.infn.it

claimed to be growing in time at high Reynolds number, due to the generation of small vortices during strong vortex–vortex interactions. The agreement between the scaling theory and the simulations was attributed to the limited Reynolds number achieved in the pseudospectral or finite-difference calculations and in the experiments, with the observation of a different behavior in simulations performed with contour-surgery methods, which were claimed to represent the evolution at higher Reynolds number. In the following years, the issue remained unresolved.

In this work we reconsider this problem, and analyze numerical solutions of two-dimensional turbulence integrated on a doubly periodic domain at very high resolution and at high Reynolds number. In the following, we study the low-order statistical moments of the velocity and vorticity fields, the probability distributions of the main quantities characterizing the vortex population, such as the total number of vortices and the distributions of vortex radii, circulations, and vorticity amplitudes, and the time evolution of the average values. The temporal scaling of the solution indicates that the peak vorticity of the vortices is constant, and that the number of vortices decays in time as predicted by the scaling theory of Carnevale *et al.*, with no evidence of a growth of the population of small vortices. In addition, this work provides evidence for a self-similar shape of the probability distributions of vortex radius and circulation. While such scaling distributions have been seen in lower Reynolds number solutions with broad-band initial conditions, this is the first case where narrow-band initial conditions evolve into vortex populations with self-similar distributions of radius and circulation.

The article is organized as follows. In Sec. II we introduce the equations of two-dimensional turbulence and two numerical solutions at different Reynolds number (i.e., different resolution and viscosity coefficient). Low-order statistical moments of the turbulent flow and one-point vorticity and velocity distributions are analyzed in Sec. III. In Sec. IV we discuss the temporal evolution of the probability distribution of vortex properties and of their average quantities. The instantaneous probability distributions of vortex properties, providing evidence for self-similarity in the distributions of vortex radius and circulation, are considered in Sec. V. Section VI gives conclusions and perspectives.

II. DYNAMICS OF DECAYING TWO-DIMENSIONAL TURBULENCE

The Navier–Stokes equations for a two-dimensional, incompressible, freely-decaying flow are written as

$$\frac{\partial \omega}{\partial t} + J[\psi, \omega] = D, \tag{1}$$

where $\omega = \nabla^2 \psi$ is vorticity, ψ is the streamfunction, and J is the two-dimensional Jacobian operator,

$$J[\psi, \omega] = \frac{\partial \psi}{\partial x}\frac{\partial \omega}{\partial y} - \frac{\partial \psi}{\partial y}\frac{\partial \omega}{\partial x}.$$

D represents a generic dissipation term due to either molecular or eddy viscosity. Here we use the form

$$D = (-1)^{n-1} \nu_n \nabla^{2n} \nabla^2 \psi, \tag{2}$$

where $n=1$ for a standard Newtonian dissipation and $n>1$ for so-called hyperviscosity. In the solutions below we use $n=2$, i.e., a biharmonic hyperviscosity. This choice allows for confining momentum dissipation at the smallest scales and for reaching higher effective Reynolds numbers at a given resolution. At high resolution, the use of hyperviscosity does not significantly affect the statistical properties of the flow on scales larger than the dissipative range. At low resolution, hyperviscous diffusion with $n \gg 1$ can lead to lack of accuracy in vortex profiles and to the formation of spurious spike-like structures near the vortex centers.[18]

The mean kinetic energy per unit area E and the mean enstrophy Z are defined by

$$E = \frac{1}{2(2\pi)^2} \int (\nabla \psi)^2 \, dx \, dy, \tag{3}$$

$$Z = \frac{1}{2(2\pi)^2} \int (\nabla^2 \psi)^2 \, dx \, dy, \tag{4}$$

where we have considered a square domain with size 2π.

Both energy and enstrophy are conserved in the inviscid case ($\nu=0$); their simultaneous conservation induces a direct cascade of enstrophy from large to small scales and an inverse cascade of energy from small to large scales.[19] Energy conservation is recovered in the limit $\nu \to 0$, since enstrophy is bounded by its initial value. In the same limit, vorticity gradients are amplified with the formation of thin filaments that are stretched until they reach the dissipation scale, so that enstrophy and all positive-order vorticity moments decay.

The first stage of the evolution, including the emergence of coherent structures, is characterized by maximum enstrophy dissipation. Once formed, vortices tend to axisymmetrize. It is worth mentioning that there is an open debate on vortex axisymmetrization. Whenever Newtonian viscosity or hyperviscosity are used, the currently achieved resolution indicates a tendency toward vortex axisymmetrization, suggesting a tendency of isolated vorticity patches to reach a local stationary solution of the equations of motion. By contrast, the use of dissipation schemes based on predetermined mechanisms of vorticity reconnection, such as contour surgery, leads to vortex shapes that do not necessarily tend to an axisymmetric shape.[20]

Since any axisymmetric structure is an exact steady solution of the inviscid equations of motion, for approximately axisymmetric vortices there is no nonlinear enstrophy transfer within vortex cores, and therefore no cascade.[5,21] Axisymmetric vortex cores are protected from deformation, dissipation, and cascade even during close interactions, when vorticity filaments are generated from the edge of the structures.[22,23] Thus, in the intermediate, vortex-dominated evolution stage, it is mainly the area outside the vortex cores that actively participates in the cascade. The vortices keep an indirect, albeit important, role in enstrophy transfer, by stretching and folding the vorticity filaments emitted during the strong vortex–vortex interactions. The filaments are

characterized by low energy and high values of the turbulent strain,[24,25] rapidly reaching the dissipation scale where they are eliminated.[17]

Using classical scaling arguments, Batchelor[26] predicted an enstrophy decay rate $Z(t) \propto t^{-2}$. The derivation is based on the observation that in the limit of high Re the energy is the only conserved quantity whereas even positive-order vorticity moments decay like $\langle |\omega|^{\alpha} \rangle \sim t^{-\alpha}$, where α is the order of the moment (e.g., $\alpha=2$ for enstrophy). Energy is predicted to cascade upscale and the theory applies only to unbounded flows or to intermediate stages of the evolution when the ratio between the energy containing scale and the domain size is much smaller than one. Important implications of Batchelor's hypothesis are the self-similar form of the one-point vorticity density and the prediction that it narrows continuously with time because of the enstrophy decay. On the contrary, velocity statistics are fixed by the value of the energy and they are approximately invariant.

Past numerical studies, however, have indicated that the self-organization of an initially random vorticity field into a collection of vortices induces a depletion of nonlinearities inside vortex cores and a considerable slowing down of the enstrophy decay rate.[21] Carnevale *et al.*[14] suggested that the classic similarity theory fails because a second asymptotic invariant appears when coherent structures emerge. In particular, these authors noted that the vorticity amplitude inside the cores of coherent vortices is conserved, and it is the main reason for the slow-down of the enstrophy decay.

The scaling theory of Carnevale *et al.* provides predictions on the evolution of the mean vortex properties and the lower statistical moments of the vorticity field, assuming that vorticity is concentrated inside coherent structures. The statistical properties of the vortex population are described in terms of the vortex number N, the average vortex radius r_a, the average vortex circulation Γ_a, and the average vorticity peak ζ_a of the vortices. As suggested by the results of the numerical simulations, the time evolution of the vortex number is assumed to have a power-law form

$$N(t) = N(t_0)\left(\frac{t}{t_0}\right)^{-\xi}. \tag{5}$$

As a further hypothesis, it is assumed that the time evolution of the probability distribution functions of vortex properties is self-similar. This allows for expressing the average of powers of dynamical quantities as powers of the averages, and for deriving from Eq. (5) the time evolution of the other average quantities by using the relationships

$$\begin{aligned} &E(t) \sim N\zeta_a^2 r_a^4 \sim \text{const}, \\ &Z(t) \sim N\zeta_a^2 r_a^2 \sim Z(t_0)\left(\frac{t}{t_0}\right)^{-\xi/2}, \\ &\Gamma_a(t) \sim \zeta_a r_a^2 \sim \Gamma_a(t_0)\left(\frac{t}{t_0}\right)^{\xi/2}. \end{aligned} \tag{6}$$

A fit of the results of a numerical simulation (corresponding to our low Re case) to the vortex decay (5), found $\xi \approx 0.72$.[14,15]

Finally, both the scaling theory of Carnevale *et al.* and the classic similarity theory are strictly valid only in the limit $\mathrm{Re} \to \infty$. For finite Reynolds number, diffusive corrections can be taken into account.[15]

Experimental confirmation of the temporal scaling behavior of decaying 2D turbulence has been obtained by Tabeling *et al.*[16] More recently, the numerical study of Clercx *et al.*[27] has considered the behavior of turbulent solutions in square containers with no-slip boundary conditions. Analyzing an ensemble of runs with $\mathrm{Re}=1000-2000$, an intermediate decay range from $t=0.2\sqrt{\mathrm{Re}}$ to $t=3\sqrt{\mathrm{Re}}$ (in nondimensional units) was detected, with $N(t) \simeq t^{-0.7\pm0.1}$. It must be noted, however, that more limited agreement was found with the other scaling exponents. At later times, the situation changes and the vortex decay rate increases. This late evolution stage can be due to the fact that energy has reached the largest scales in a domain with no-slip boundaries; vortices are substantially weakened after strong vortex–wall interactions and may then be dissipated faster.

Most of the above results refer, however, to situations where the Reynolds number is quite moderate. Soon after the scaling theory of Carnevale *et al.* was developed, the criticism was raised that this scaling theory is appropriate only for low Re where diffusion is still a dominant effect, while it loses its validity at larger Reynolds number.[17] One way to address this issue, and the one that is followed here, is to perform numerical simulations at much larger Re (although, of course, not infinitely large). If the basic result of a power-law decay of the vortex number found at lower resolution still holds at larger Reynolds number, then this supports the view that a scaling theory correctly captures the high Re behavior.

III. GLOBAL PROPERTIES OF 2D TURBULENCE AT HIGH REYNOLDS NUMBER

In the present work, the 2D Navier–Stokes Eq. (1) is integrated by using a parallel, fully implicit multigrid elliptic solver. The time discretization is based on a Crank–Nicholson scheme. The second-order spatial discretization follows an Arakawa scheme on a nonstaggered grid. The fluid evolves in a periodic square box of size $2\pi \times 2\pi$.

We consider two solutions. One is a high Reynolds number solution, with resolution 4096^2 grid points and hyperviscosity coefficient $\nu_2 = 9.53 * 10^{-13}$. The second is a lower Reynolds number simulation with resolution 512^2 and hyperviscosity $\nu_2 = 3.5 \times 10^{-9}$. This latter value was used by Weiss and McWilliams,[15] in a pseudospectral numerical integration. A typical vortex at time $t=6$ spans approximately 16 grid points in the high-Re simulation and 6 points in the low-Re simulation.

The initial conditions are given by a zero mean, Gaussian vorticity field with random Fourier phases. At both resolutions, the initial energy spectrum is narrow-band and it is given by $E(k) = C_0 k^6 / [(1 + k/60)^{18}]$, where C_0 is a normalization constant. The spectrum is peaked at wave number $k_0 = 30$. The initial vorticity field has kinetic energy $E(t=0) = 0.5$ and averaged enstrophy $Z(t=0) = 2200$, which implies a typical eddy-turnover time $t_e = Z^{-1/2} \approx 0.021$. Com-

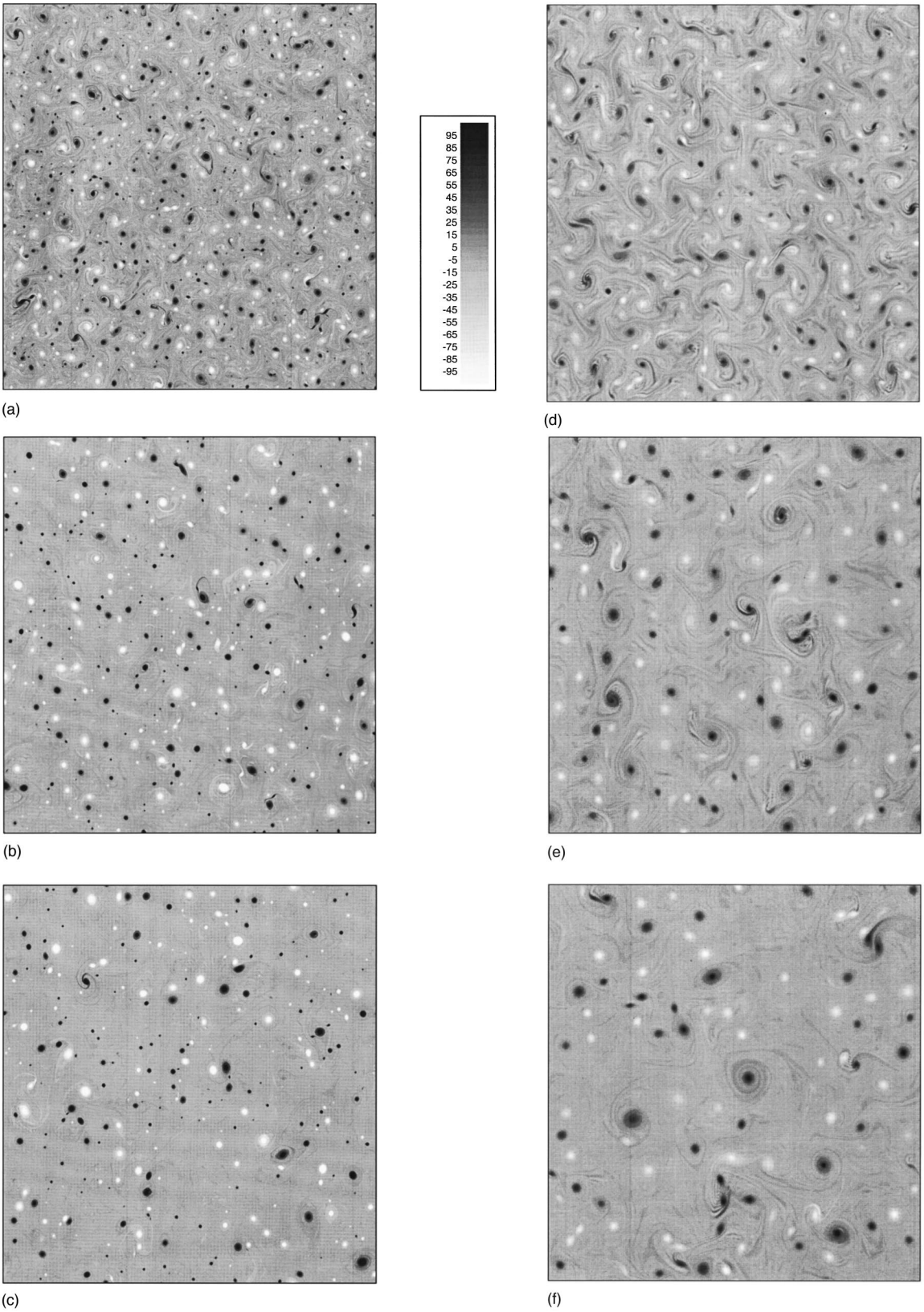

FIG. 1. Panels (a)–(c) show the vorticity field for the simulation at high-Re (resolution 4096^2) at times $t=3$, 7, 11. Panels (d)–(f) show the vorticity field for the simulation at moderate Re (resolution 512^2) at the same times, starting from the same random initial conditions. Note the different number of vortices in the two cases.

paring the high- and low-resolution cases, we see that the former corresponds to ''opening'' the availability of small scales (high wave numbers) to the dynamical evolution, without initially introducing energy at the small scales.

For both values of the Reynolds number considered here, the evolution of the system leads to the presence of coherent structures, whose emergence is completed by the time $t \approx 2$. In the high resolution case, a large number of well-formed, small-scale vortices surrounded by low-vorticity filaments can be observed already at time $t=3$, see Figs. 1(a) and 1(d). A smaller number of vortices is present in the lower resolution simulation. (Note the presence of numerically-generated wiggles in the low-Re simulation. Here, we used the same viscosity employed by Weiss and McWilliams.[15] However, since we employ a finite-difference code, no spectral dealiasing is implemented and small-scale wiggles due to the computational mode can be generated. These, however, do not affect the properties of the field at larger scales, as shown by performing simulations with slightly larger viscosity that provide analogous statistics.) In both cases, dipoles of opposite-sign vortices and merging interactions between vortices of the same sign characterize the dynamics, resulting in a slow growth of the average vortex size and a decrease of the total number of coherent structures as time progresses [compare for example Figs. 1(b)–1(c) and 1(e)–1(f)]. In the simulations at higher Reynolds number, the number and the amplitude of the vortices is definitely larger, with a considerable amount of small structures that cannot be observed at lower Reynolds number.

We next consider the global statistical properties of the flow. First we concentrate on the second-order moments $E(t)$ and $Z(t)$, shown in Fig. 2. In the high-Reynolds number case, 0.4% of the initial kinetic energy is dissipated during the evolution from $t=0$ to $t=11$. In the low-resolution experiment, dissipation is much larger and 10.8% of the energy is lost.

In our simulations, the enstrophy decay is much slower than the t^{-2} law deduced from classical arguments. After the initial transient phase, the slope is consistent with the scaling theory prediction with $\xi=0.72$, obtained by Weiss and McWilliams[15] analyzing a long-time integration of Eq. (1) and a modified point vortex model. The high-resolution simulation at $t \geqslant 3$ provides a noticeable improvement compared to the 512^2 case.

The energy power spectra from time $t=1$ to $t=11$ are shown in Fig. 3. Energy is primarily transferred to large scales and the occurrence of coherent structures induces a spectral slope at small scales that is steeper than the k^{-3} cascade predicted by classical similarity theories. Note that during the time interval considered here, the energy spectrum is not strongly peaked at $k=1$, indicating that the domain size is still unimportant.

The one-point vorticity probability density functions (PDFs) are shown in Fig. 4. In the high Reynolds number case [Fig. 4(a)] the central core of the distribution narrows significantly with time. Correspondingly, filaments in the background are stretched and dissipated. The tails of the distribution, however, are almost invariant. The invariance of the tails in the distribution indicates that the high-vorticity

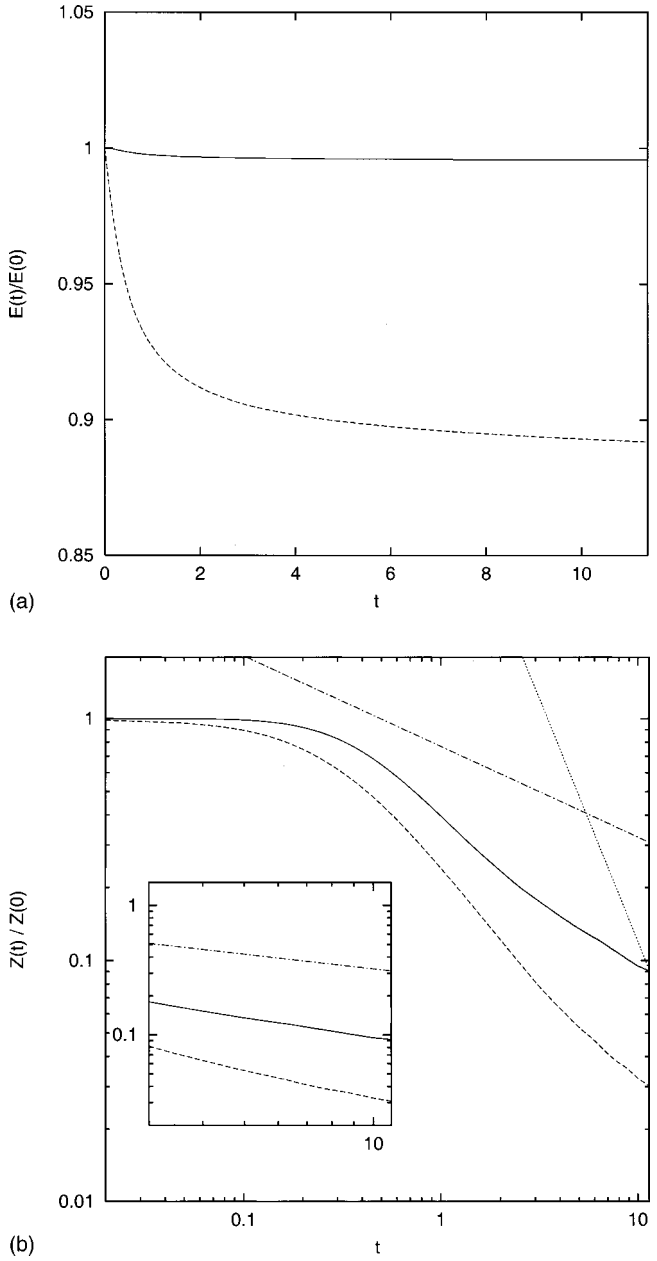

FIG. 2. Panel (a) shows the normalized mean kinetic energy $E(t)/E(0)$ for the simulation at high-Re (solid line) and for that at moderate-Re (dashed line). Panel (b) shows the normalized mean enstrophy $Z(t)/Z(0)$ for the same two simulations. Predictions from classic scaling arguments (dotted line) and from the scaling theory of Carnevale *et al.* (dashed-dotted line) are also shown. The inset shows the normalized mean enstrophy and the scaling theory prediction from time $t=3$ to $t=11$.

levels, typical of the cores of the most intense vortices, are nearly conserved, in agreement with the scaling theory hypothesis. Note also that past simulations[4,28] did not fully reveal the invariance of the tails at high vorticity. This characteristic is revealed here due to the high Reynolds number achieved.

The velocity distribution (Fig. 5) is clearly non-Gaussian, with pronounced tails that are approximately described by an exponential distribution. It has been noted[9,10] that non-Gaussian velocity PDFs with approximately exponential tails characterize high-Re two-dimensional turbulent

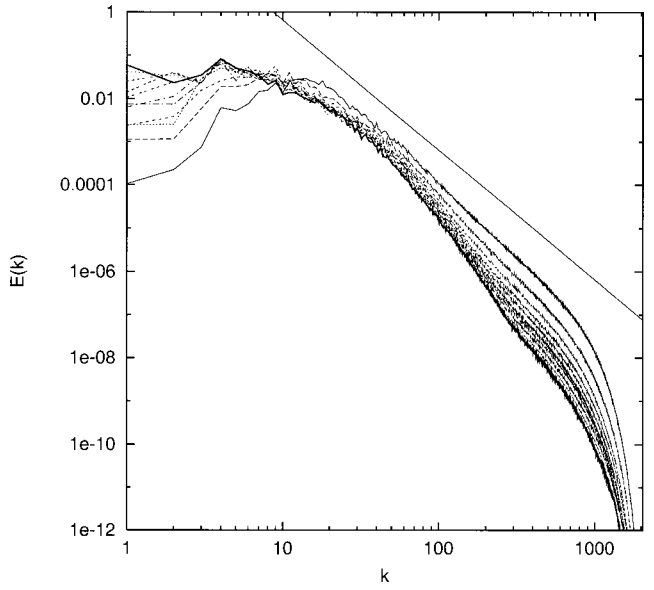

FIG. 3. Energy spectra for the solution at high Re for times $t=1,2,...,11$. Solid line shows the k^{-3} classical prediction.

flows when the dynamics is controlled by strongly peaked vortices with small radius. In this case, the properties of the velocity field are determined by the characteristics and the shape of the vortices, not only in regions close to the vortices but everywhere. As in point-vortex systems, the velocity distribution of 2D turbulent flows is dominated by the far-field velocity component induced by the coherent vortices. In the presence of small strong vortices, the far-field velocity component generated by the vortices is non-Gaussian.

IV. TEMPORAL SCALING BEHAVIOR OF THE VORTEX POPULATION

In the present work, coherent vortices are identified by the vortex census algorithm discussed by McWilliams.[4] Local vorticity concentrations are selected and tested; only connected domains of high vorticity that are monotonically decreasing from a central extremum with an approximately axisymmetric shape are recognized as vortices.

Figure 6(a) shows the time evolution of the total number of vortices $N(t)$ for the two values of the Reynolds number considered. The integration for the higher Re value reaches the (nondimensional) time $t=11$, while the solution at lower Re proceeds until time $t=20$.

Two facts emerge from this figure. First, the total number of vortices is not the same in the two simulations, with a much larger number of vortices in the case at high Re. When filtering the high-resolution simulation once vortices have formed (at, say, $t=5$), and reducing it to the same resolution used in the low-Re case, the number of vortices does not change much, indicating that most of these high-Re vortices, once formed, are large enough to survive also at lower resolution. We have also evolved a low-Re case until vortex formation was over (again, $t=5$), and then ''upgraded'' it to resolution 4096^2 and correspondingly higher Re, evolving it further. The population of vortices remained that of the low-Re case, and the filaments emitted during strong vortex

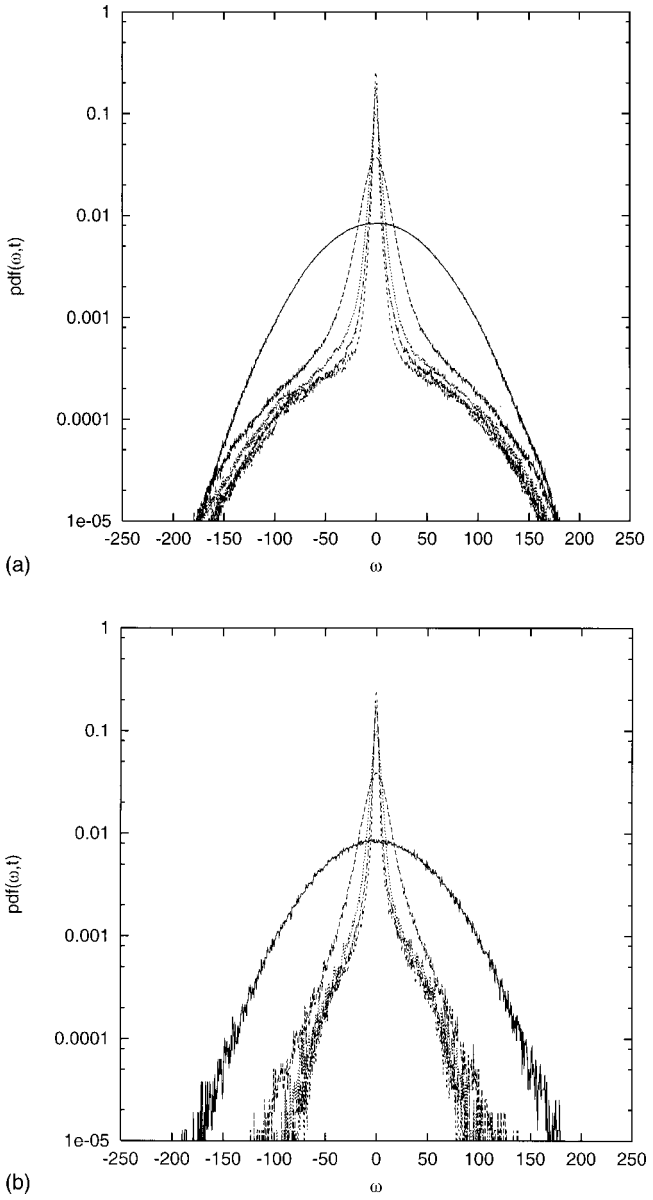

FIG. 4. Panel (a) shows the vorticity distribution for the high-Re solution at times $t=0$, $t=2$ (dashed line), $t=5$ (dashed-dotted line), $t=8$ (dotted line), and $t=11$ (solid line). Panel (b) shows the vorticity distribution for the low-Re solution at the same times.

interactions did not roll up into new small-scale vortices. Taken together, these results indicate that the vortex generation process is sensitive to the value of the Reynolds number, with a larger number of vortices formed at high Re, even starting from the same initial conditions. From the inspection of the time evolution of the vorticity field, we have noted that in the initial incoherent phase enstrophy is rapidly transferred to the smaller scales, down to the dissipative range, where vortex generation starts to occur. With the initial conditions employed here, vortices are born at the smallest scales where advection dominates over dissipation, subsequently growing by merging events. In the evolution from a random Gaussian initial field to a vortex-dominated system, the dissipation thus sets the lower limit to the size and the amplitude of the vortices that are generated. The larger the Reynolds number, the more numerous, smaller, and more

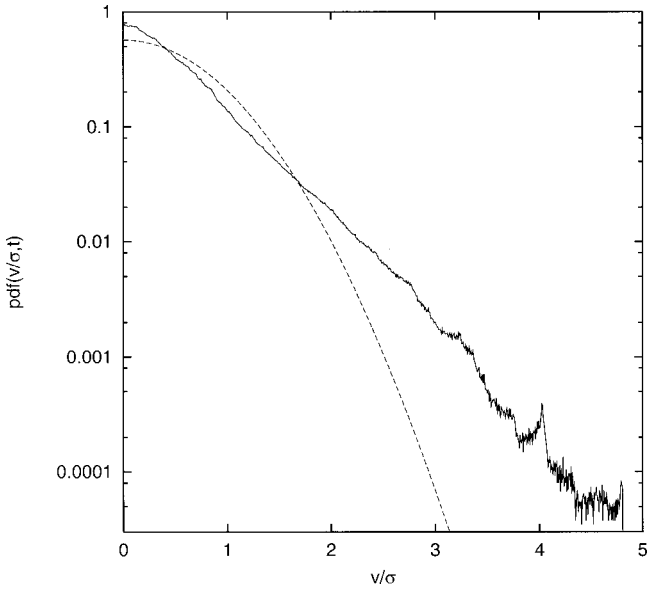

FIG. 5. Velocity distribution at time $t=11$ for the solution at large Reynolds number.

intense are the vortices generated during this initial stage. Presumably, this is because in the time interval preceeding vortex generation the vorticity peaks that will evolve into coherent vortices are dissipated much less in the high-Re case, surviving until they become part of a coherent vortex. As a consequence, this initial stage is definitely sensitive to the value of the Reynolds number.

After the vortices have been generated and the system has become dominated by vortex dynamics, the situation changes. The intermediate regime, for which the scaling theory of Carnevale *et al.* has been proposed, is the focus of the present study. In Fig. 6(a) we show the number of vortices as a function of time for the two simulations considered, together with the power-law decay with the exponent $\xi=0.72$ proposed by Weiss and McWilliams.[15] A least-square-fit estimate of the vortex decay rate at high Reynolds number gives $\xi=0.76\pm0.03$, where the indicated uncertainties are the 63.8% confidence limits. We also compute the minimum and maximum estimates to the decay exponent as given by a ''jackknife'' approach, consisting in making estimates of the decay exponent by dropping one point at random in the set of values to be least-square-fitted. These give respectively $\xi_{\min}=0.73\pm0.02$ and $\xi_{\max}=0.77\pm0.02$.

In Fig. 6(b) we show the time evolution of the average vortex circulation Γ_a, the average vortex radius r_a, and the average modulus of the vorticity peak ζ_a inside vortex cores, for the solution at higher Re. The predictions of the scaling theory, corresponding to $\xi=0.72$, are shown as solid lines. Table I reports the least-square fits to the scaling exponents together with the 63.8% confidence limits and the minimum and maximum jackknife estimates.

The least-square-fit values reported in Table I for the vortex radius and circulation reveal an interesting discrepancy with the scaling theory of Carnevale *et al.* A possible explanation of this discrepancy is suggested by careful inspection of Fig. 6(a). Here, some deviations from scaling

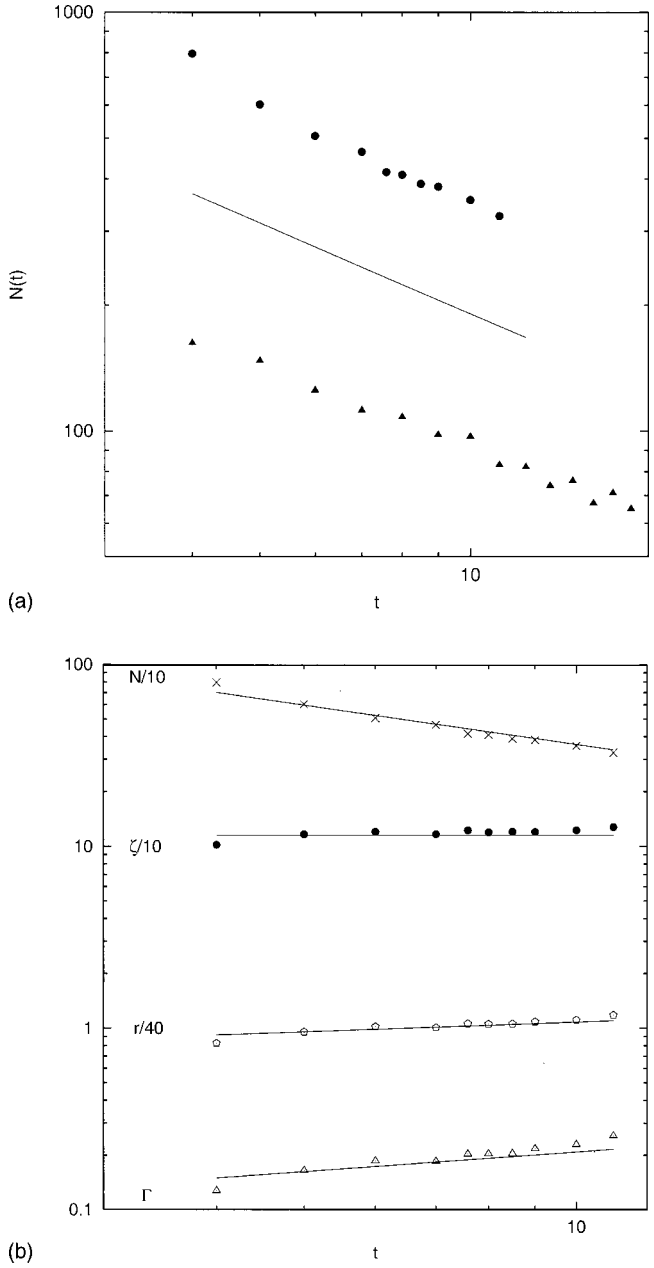

FIG. 6. Panel (a) shows the time evolution of the vortex number at high-Re (circles) and low-Re (triangles). The prediction of the scaling theory with $\xi=0.72$ is shown as a solid line. Panel (b) shows the time evolution of the vortex number (crosses), the average vorticity peak magnitude ζ_a (dots), the average vortex radius r_a (pentagons), and the average vortex circulation magnitude Γ_a (triangles) for the simulation at large Reynolds number. Solid lines show the slopes predicted by the scaling theory with $\xi=0.72$.

behavior are observed at times $t=4$, 5, where the decay is slightly faster than predicted. This deviation is associated with the presence of a population of small, weaker vorticity patches that are dissipated faster than the stronger vortices, and can be considered a transient phase that is still influenced by the vortex generation processes.

Figure 7 shows the modulus of the vorticity amplitude of each coherent vortex versus its radius, for two different times in the evolution, for the high Re solution. Two different populations of vortices emerge from these plots. These consist of a population of small vortices with amplitude weaker

TABLE I. Decay exponents of vortex statistics in the high-Re simulation for the whole vortex population. The first column indicates the quantity considered; the second column shows the result of the least-square fit on the time interval $5 \leqslant t \leqslant 11$ together with the 63.8% confidence limits; the third and fourth columns show the minimum and maximum estimates as obtained by a jackknife method.

Quantity	Least-square fit	Min estimate	Max estimate
N^{-1}	0.76 ± 0.03	0.73 ± 0.02	0.77 ± 0.02
ζ_a	0.09 ± 0.02	0.06 ± 0.02	0.1 ± 0.02
Γ_a^2	1.00 ± 0.09	0.90 ± 0.08	1.07 ± 0.09
r_a^4	0.94 ± 0.10	0.82 ± 0.09	1.03 ± 0.10

than the average, and of another population of stronger coherent structures with larger radius. Figure 7 also indicates that the weak vortex population is not a self-similar extension of the ensemble of strong vortices, as a definite gap is visible between them.

The comparison between the two different times shown in Fig. 7 confirms that the time evolution of the two populations proceeds differently. In particular, the population of weaker vortices is depleted more effectively than that of intense vortices. In addition, intense vortices display an almost invariant distribution of peak vorticity, consistent with the scaling theory. To quantitatively distinguish between the fates of the two populations, we separate them by setting a threshold on the vorticity amplitude. An appropriate value (as evident from Fig. 7) is $\zeta_{\mathrm{tr}} = 50$.

Figure 8 shows the time evolution of the number of strong ($|\zeta| > \zeta_{\mathrm{tr}}$) and weak ($|\zeta| < \zeta_{\mathrm{tr}}$) vortices in the high Reynolds number simulation. The decay of the number of weaker vortices is more rapid than that of the strong coherent structures, the latter displaying full agreement with the predictions of the scaling theory. Table II reports the values of the scaling exponents as obtained from least-square fits to the time evolution of the strong, coherent vortex population with $|\zeta| > \zeta_{\mathrm{tr}}$, the associated 63.8% confidence limits, and the minimum and maximum jackknife estimates. A better agreement is now observed with the scaling theory of Carnevale *et al.*, and the least-square fit uncertainties have been reduced. However, a small discrepancy is still observed for the value of the scaling exponent of the vortex circulation.

We interpret this result as indicative of the presence of a population of weak vorticity patches that are generated during the process of vortex formation from random initial conditions, and that decay rapidly. Presumably, these weaker vortices are not truly coherent structures, since they do not live long enough to be classified as coherent vortices. The deviation of the collapsing weak-vortex population behavior from the scaling theory does not contaminate our analysis at later times, since the weak-vortex population is relatively small and it decays much faster than the population of truly coherent vortices. The scaling theory then applies to this latter population of intense vortices that survive for long times.

Note, finally, that even at the higher Reynolds number considered here we do not observe the production of small vortices by instability of the filaments during vortex merging interactions. As mentioned above, by upgrading the resolution (and correspondingly lowering the viscosity) of a low-Re simulation once vortex generation is over, one observes that the vortex population remains the same as for the low-Re case, suggesting that once vortices have formed the value of the Reynolds number plays a more limited role. Of course, we cannot exclude that at still higher Re a transition occurs and other statistical properties are present, even though the fact that similar results are found at high and low resolution suggests that scaling behavior can be an important property of 2D turbulence at high Reynolds number.

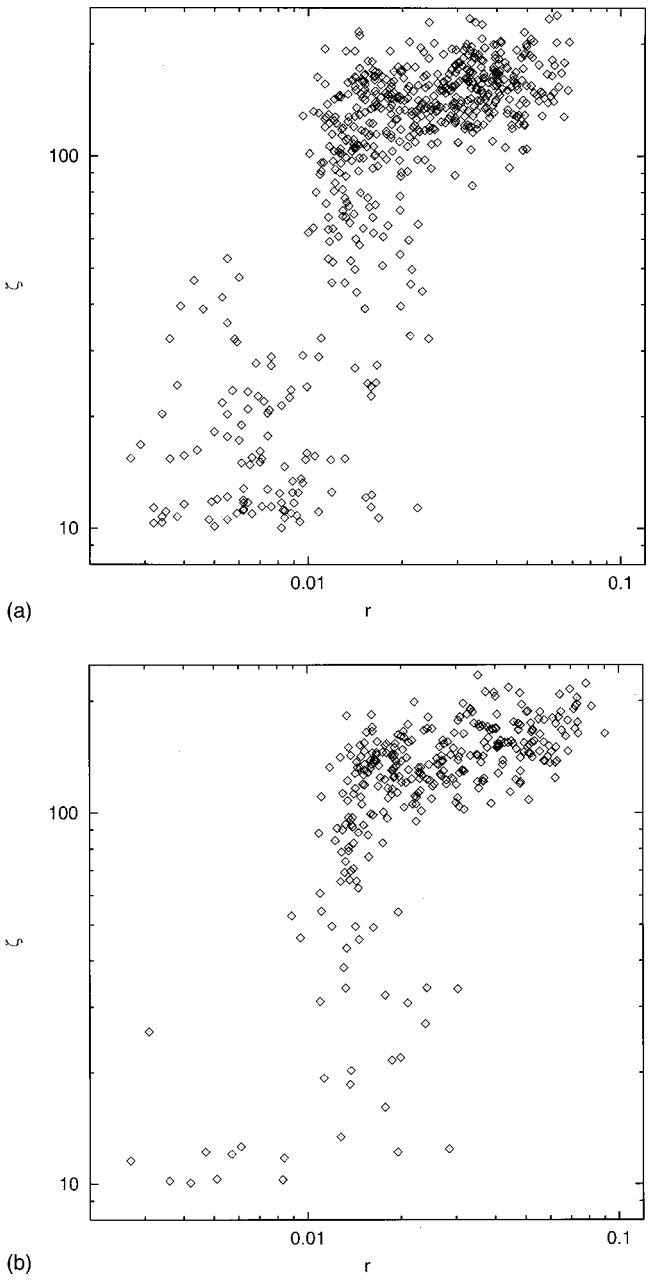

FIG. 7. Scatter plot of peak vorticity versus radius for the vortex population at high-Re, at times $t = 5$ (panel a) and $t = 11$ (panel b).

V. SELF-SIMILARITY OF THE VORTEX DISTRIBUTION

As a further test of the scaling behavior, we recall that the assumption of a self-similar evolution of the vortex properties implies that the instantaneous probability distributions

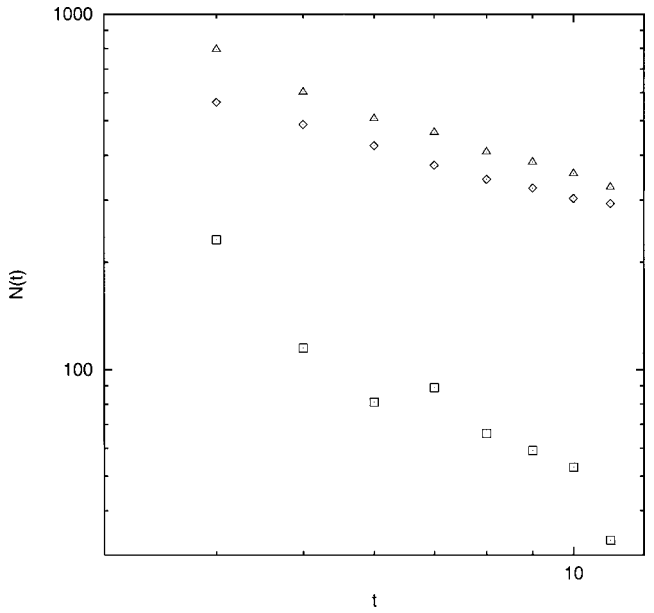

FIG. 8. Time evolution of the number of strong (diamonds) and weak (squares) vortices, compared with the evolution of the total number of vortices (triangles), for the solution at high Reynolds number.

of vortex amplitude, radius, and circulation should be independent of time when normalized to the average value at a given time, i.e., considering for example the vortex circulation Γ,

$$p(|\Gamma'(t)|)=p\left[\frac{|\Gamma(t)|}{\Gamma_a(t)}\right]=p\left[\frac{|\Gamma(t^*)|}{\Gamma_a(t^*)}\right], \tag{7}$$

where $\Gamma_a(t)$ is the average circulation at time t, and t and t^* are two times in the scaling range.

In Figs. 9(a)–9(c) we show the instantaneous distributions of the modulus of the vorticity peak, radius, and circulation for the vortex population at several times from $t=4$ to $t=11$, for the simulation at high Re. Within sampling variability, the distributions are identical, and they are consistent with the self-similarity hypothesis. For comparison, in Figs. 9(d), 9(f) we show the distributions of vorticity peak, radius and circulation for the situation of lower Re. Notwithstanding the presence of a larger sampling variability due to the smaller number of vortices, also in this case the distributions are consistent with the scaling hypothesis.

There is, however, an intriguing difference between the instantaneous distributions of the vortex properties at high and moderate Reynolds numbers. Figures 9(b) and 9(c) indicate that the instantaneous distributions of radius and circulation for the high Re case have an approximate power-law behavior. By contrast, no power law is visible in the distribution of vortex radius and circulation for the lower Reynolds number, as shown in Figs. 9(e) and 9(f).

A self-similarity of the distribution of vortex radii has been previously detected by Benzi *et al.*[29] in the analysis of freely-decaying turbulence with broad-band initial conditions and resolution comparable to our low-Re simulation. The same authors did not find any evidence of spatial self-similarity in the distribution of vortex radii for narrow-band initial conditions, consistent with the results discussed here for the low-resolution case and the results of Weiss and McWilliams[15] for 2D turbulence and point-vortices. However, here we observe that when the Reynolds number is large enough, even narrow-band initial conditions lead to spatially self-similar distributions of vortex properties. Examination of the time evolution of the flow indicates that the population of small vortices is not generated by roll-up of filaments after vortex–vortex interactions, but rather by self-organization of the small vorticity peaks at the time of vortex formation.

In Fig. 9(b) we also show the power-law fit to the distribution, as suggested by Benzi *et al.* for broad-band initial conditions. This power-law behavior is consistent with the distribution of vortex properties at high Re obtained here. The approximate agreement between these two situations, that differ in both the value of the Reynolds number and the type of initial conditions, suggests a generic nature of self-similar distributions of vortex properties at large Reynolds number. Since the rationalization of size-scaling is merger of smaller to larger vortices in a temporally stationary way, the question of end effects in numerical simulations naturally arise; i.e., what is the impact of having a finite range of sizes with no vortices larger and smaller than that range? Benzi *et al.* showed that the end effects did not affect their results for a broad-size population, and our results suggest that they are unimportant even when the size range is not too broad and the whole evolution is temporally scaling rather than stationary.

TABLE II. Decay exponents of vortex statistics in the high-Re simulation for the population of strong coherent vortices with $|\zeta|>\zeta_{tr}$. The first column indicates the quantity considered; the second column shows the result of the least-square fit on the time interval $5\leqslant t\leqslant 11$ together with the 63.8% confidence limits; the third and fourth columns show the minimum and maximum estimates as obtained by a jackknife method.

Quantity	Least-square fit	Min estimate	Max estimate
N^{-1}	0.67 ± 0.02	0.66 ± 0.03	0.70 ± 0.01
ζ_a	0.01 ± 0.01	-0.01 ± 0.01	0.02 ± 0.01
Γ_a^2	0.84 ± 0.04	0.80 ± 0.05	0.85 ± 0.03
r_a^4	0.68 ± 0.04	0.64 ± 0.05	0.70 ± 0.04

VI. CONCLUSIONS

In this work we have numerically studied the evolution of vortex statistics in freely-decaying two-dimensional turbulence at very large Reynolds number. At intermediate times, the evolution of the low order moments of the turbulent flow and the decay of the vortex number display a temporal scaling behavior consistent with the scaling theory of Carnevale *et al.*[14] The global statistical properties, namely the one-point vorticity and velocity distributions and the instantaneous distributions of vortex properties, confirm the basic assumptions of the theory on the conservation of the vorticity amplitude inside vortex cores and on the temporal evolution of the vortex population. The average vortex radius and circulation for the strong-vortex population decay as power laws with an exponent close to that predicted by the scaling theory, although a small discrepancy is observed for the value of the

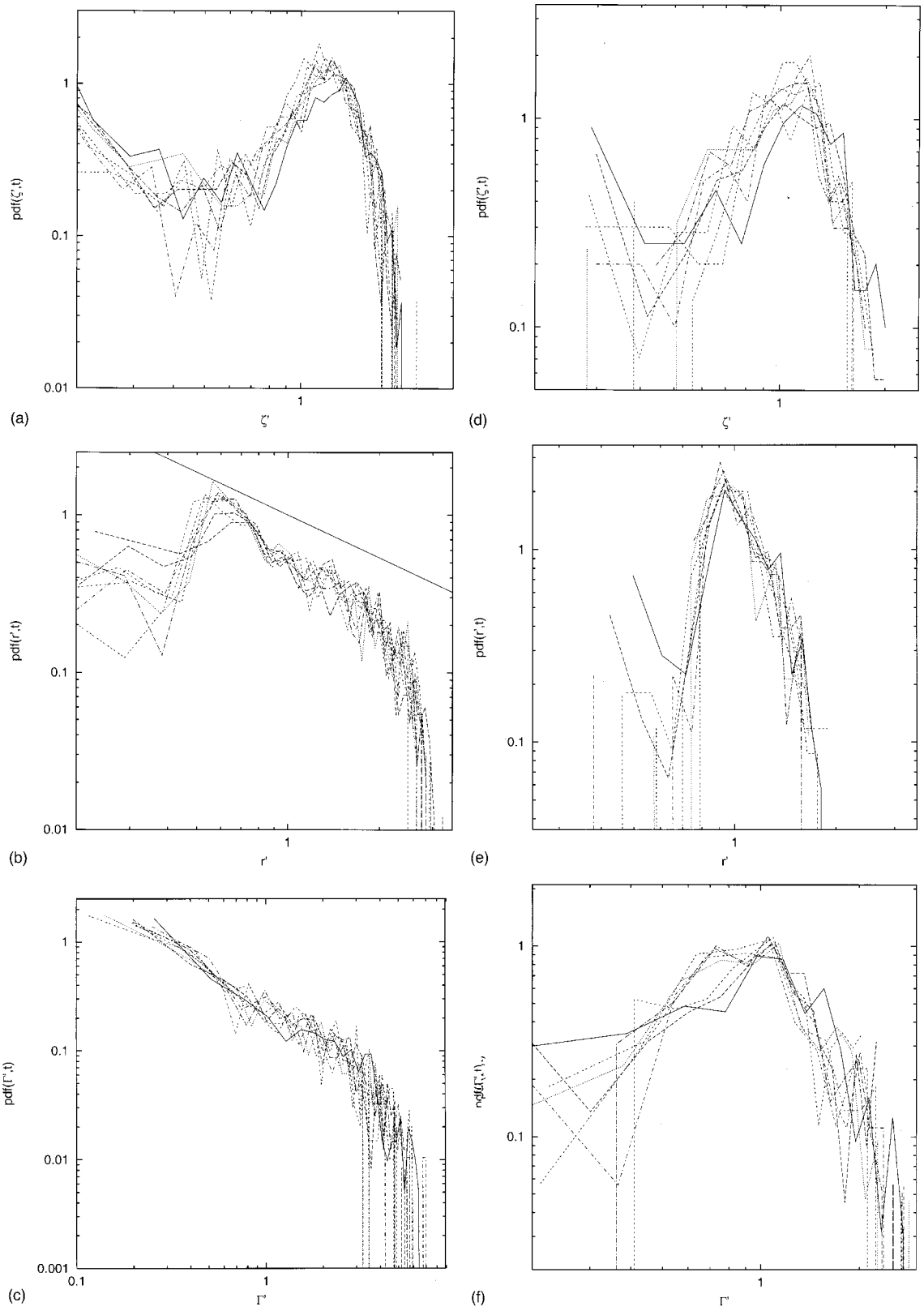

FIG. 9. Panels (a)–(c) show the instantaneous distributions of normalized peak vorticity $|\zeta'|$, vortex radius r' [the full line has a slope -0.90 as suggested by Benzi *et al.* Ref. 29] and circulation Γ' for the high-Re turbulent solution at times $t=4,5,6,...,11$. Panels (d)–(f) show the instantaneous distributions of normalized peak vorticity, vortex radius, and circulation for the solution at low-Re.

exponent for the circulation. Note, also, that no generation of small-scale vortices after strong vortex interactions is observed, contrary to the earlier claims of Dritschel.[17]

Overall, the results discussed in this work indicate that scaling theories such as those developed by Carnevale *et al.*,[14] Weiss and McWilliams,[15] Riccardi *et al.*,[30] and Sire and Chavanis,[31] based on a simplified description of the vortex interactions, provide a good description of the dynamics during the intermediate, vortex-dominated evolution stage. In particular, scaling theories appear to be able to capture most of the relevant aspects of the behavior of freely-decaying two-dimensional turbulence at large Reynolds numbers. It is also interesting to note that average vortex quantities show a similar temporal evolution for both values of the Reynolds number considered here. This suggests that already at lower resolution (512^2), scaling theories provide a proper description of the turbulent dynamics, and that some of the average properties of two-dimensional turbulence can already be studied at moderate resolution.

In addition, we have obtained evidence for a self-similar distribution of vortex radii and circulations even for narrow-band initial conditions, partially confirming the size-scaling theory proposed by Benzi *et al.*[29] and suggesting the possible existence of a generic statistical behavior of the decaying phase of two-dimensional turbulence at high Reynolds number.

Clearly, the results reported here are in contrast with the earlier findings of Dritschel[17] that were based on the use of a contour surgery approach. The discrepancy with the results of Dritschel[17] remains unexplained. One possibility is that contour surgery possesses a superior performance compared to any other numerical scheme, that makes it capable of capturing the turbulent behavior at much larger Reynolds number that the one achieved in any simulations using Newtonian viscosity or hyperviscosity. Alternatively, the discrepancy could be due to the fundamental inability of contour surgery to properly represent Navier–Stokes dynamics.

The present work has also shown that the initial period of vortex formation, prior to the intermediate vortex-dominated stage described by the scaling theory, is definitely dependent on the value of the Reynolds number. In our opinion, the main open issue of decaying two-dimensional turbulence is the understanding of the mechanisms that lead to vortex formation starting from different types of initial conditions, and of the consequent dependence of the vortex statistics on initial conditions. We plan to address some of these issues in future studies.

ACKNOWLEDGMENTS

This work has been supported by the Grant ''High resolution simulations of 2D geophysical turbulence'' of the CINECA supercomputing center in Bologna, Italy. This article is dedicated to Clive Baillie, who participated in the early stages of this work.

[1] J. Charney, ''Geostrophic turbulence,'' J. Atmos. Sci. **28**, 1087 (1971).
[2] J. Pedlosky, *Geophysical Fluid Dynamics* (Springer, New York, 1987).
[3] J. C. McWilliams, ''The emergence of isolated coherent vortices in turbulent flow,'' J. Fluid Mech. **146**, 21 (1984).
[4] J. C. McWilliams, ''The vortices in two-dimensional turbulence,'' J. Fluid Mech. **219**, 361 (1990a).
[5] A. Babiano, C. Basdevant, B. Legras, and R. Sadourny, ''Vorticity and passive scalar dynamics in two-dimensional turbulence,'' J. Fluid Mech. **183**, 379 (1987).
[6] R. Benzi, G. Paladin, S. Patarnello, P. Santangelo, and A. Vulpiani, ''Intermittency and coherent structures in two-dimensional turbulence,'' J. Phys. A **19**, 3771 (1986).
[7] D. Marteau, O. Cardoso, and P. Tabeling, ''Equilibrium states of 2D turbulence: An experimental study,'' Phys. Rev. E **51**, 5124 (1995).
[8] P. Santangelo, R. Benzi, and B. Legras, ''The generation of vortices in high-resolution, two-dimensional decaying turbulence and the influence of initial condition on the breaking of self-similarity,'' Phys. Fluids A **1**, 1027 (1989).
[9] A. Bracco, J. LaCasce, and A. Provenzale, ''Velocity pdf's for oceanic floats,'' J. Phys. Oceanogr. **30**, 461 (2000).
[10] A. Bracco, J. LaCasce, C. Pasquero, and A. Provenzale, ''The velocity distribution of barotropic turbulence,'' to appear in Phys. Fluids.
[11] R. Benzi, S. Patarnello, and P. Santangelo, ''On the statistical properties of two-dimensional decaying turbulence,'' Europhys. Lett. **3**, 811 (1987).
[12] D. G. Dritschel, ''A general theory for two-dimensional vortex interactions,'' J. Fluid Mech. **293**, 269 (1995).
[13] W. Matthaeus, W. Stribling, D. Martinez, S. Oughton, and D. Montgomery, ''Decaying two-dimensional Navier-Stokes turbulence at very long times,'' Physica D **51**, 531 (1991).
[14] G. F. Carnevale, J. C. McWilliams, Y. Pomeau, J. B. Weiss, and W. R. Young, ''Evolution of vortex statistics in two-dimensional turbulence,'' Phys. Rev. Lett. **66**, 2735 (1991).
[15] J. B. Weiss and J. C. McWilliams, ''Temporal scaling behavior of decaying two-dimensional turbulence,'' Phys. Fluids A **5**, 608 (1993).
[16] P. Tabeling, S. Burkhart, O. Cardoso, and H. Willaime, ''Experimental study of freely decaying two-dimensional turbulence,'' Phys. Rev. Lett. **67**, 3772 (1991).
[17] D. G. Dritschel, ''Vortex properties of two-dimensional turbulence,'' Phys. Fluids A **5**, 984 (1993).
[18] A. Mariotti, B. Legras, and D. G. Dritschel, ''Vortex stripping and the erosion of coherent structures in two-dimensional flows,'' Phys. Fluids A **6**, 3954 (1994).
[19] R. H. Kraichnan, ''Inertial ranges in two-dimensional turbulence,'' Phys. Fluids **10**, 1417 (1967).
[20] D. G. Dritschel, ''On the persistence of non-axisymmetric vortices in inviscid two-dimensional flows,'' J. Fluid Mech. **371**, 141 (1998).
[21] J. C. McWilliams, ''A demonstration of the suppresion of turbulent cascades by coherent vortices in two-dimensional turbulence,'' Phys. Fluids A **2**, 547 (1990b).
[22] M. V. Melander, J. C. McWilliams, and N. J. Zabuski, ''Axisymmetrization and vorticity-gradient intensification of an isolated two-dimensional vortex through filamentation,'' J. Fluid Mech. **178**, 137 (1987).
[23] J. von Hardenberg, J. McWilliams, A. Provenzale, A. Shchepetkin, and J. B. Weiss, ''Vortex merging in quasigeostrophic flows,'' J. Fluid Mech. **412**, 331 (2000).
[24] A. Okubo, ''Horizontal dispersion of floatable particles in the vicinity of velocity singularities such as convergences,'' Deep-Sea Res. **17**, 445 (1970).
[25] J. Weiss, ''The dynamics of enstrophy transfer in two-dimensional turbulence,'' Physica D **48**, 273 (1991).
[26] G. Batchelor, ''Computation of the energy spectrum in homogeneous two-dimensional turbulence,'' Phys. Fluids Suppl. **12**, 233 (1969).
[27] H. J. H. Clercx, S. R. Maassen, and G. J. F. van Heijst, ''Decaying two-dimensional turbulence in square containers with no-slip or stress-free boundaries,'' Phys. Fluids A **11**, 611 (1999).
[28] P. Bartello and T. Warn, ''Self-similarity of decaying two-dimensional turbulence,'' J. Fluid Mech. **326**, 357 (1996).
[29] R. Benzi, S. Patarnello, and P. Santangelo, ''Self-similar coherent structures in two-dimensional decaying turbulence,'' J. Phys. A **21**, 1221 (1988).
[30] G. Riccardi, R. Piva, and R. Benzi, ''A physical model for merging in 2D decaying turbulence,'' Phys. Fluids A **7**, 3091 (1995).
[31] C. Sire and P.-H. Chavanis, ''Numerical renormalization group of vortex aggregation in 2D decaying turbulence: the role of three-body interactions,'' Phys. Rev. E (submitted).